Intake systems in ephemeral rivers

L. G. Castillo, J. T. García & J. M. Carrillo
Department of Civil Engineering,
Technical University of Cartagena, Spain

Abstract

This paper is focused on the study of bottom rack intake systems located in ephemeral and torrential streams. Clear water, and water with gravel sediment transport have been analyzed. Different tests have been carried out to quantify the influence of the solids passing through the racks. The wetted rack lengths and the efficiency of racks are studied. The clear water has also been modelled with computational fluid dynamics, and compared with the measurements obtained in the laboratory. Experimental and numerical studies that characterize both the clear water and the influence of solid load in the operation of the bottom racks will allow us to improve the existing design criteria.
Keywords: bottom racks, intake system, gravels, laboratory measurements, sediment transport, CFD.

1   Introduction

Bottom rack intake systems are used to collect the maximum quantity of water on small, steeply sloping mountain rivers with important sediments transport.

Due to the fact that the bed load sediment transport passes over the racks, they have to operate under extreme conditions (Bouvard [1]).

Most design recommendations try to avoid rack occlusion. Some of them are based on prototype measurements. The main parameters are:

- The bar clearance, which must be higher than the biggest grain sizes transported during floods.
- The longitudinal rack slope. The increase in the rack slope tends to reduce the probability of sediment load over it.
- The percentage of increment in the opening area of the rack by the consideration of the surface partially clogging.

- The construction of an upstream stilling basin, which regulates the size of the incoming sediments.

Based on intake systems located in the French Alps, Ract-Madoux *et al.* [2] proposed a bar clearance near 0.100 m and a longitudinal rack slope near 20%.

Using Tyrolean weirs of Tiroler Kraftwerke AG, Simmler [3] and Drobir [4], recommend to use a bar clearance around 0.150 m, with $d_{95} \approx 0.060$ m, a longitudinal rack slope between 20 and 30%, and a rack opening area increment factor from 1.5 to 2.0. Based on the same bottom intakes systems as Ract-Madoux *et al.* [2], Bouvard [1] considered a bar clearance close to 0.100–0.120 m (0.020–0.030 m in the case of intake systems for power plants), rack slopes between 30 and 60%, and rack opening area factor between 1.5 and 2.0. Raudkivi [5] recommended a minimum bar clearance of 0.005 m for a longitudinal rack slope near 20%. The shape of the bars has also been analyzed to determine the amount of derived flow (Orth *et al.* [6], Frank [7], Noseda [8], Drobir [4], Drobir *et al.* [9], Bouvard [1]).

Experimental and numerical studies are currently focused on the analysis of solids passing over bottom racks. Ahmad and Kumar [10] studied in the laboratory the percentage of solids passing through the rack. The authors considered the longitudinal rack slope, different water flows, and the ratio between the size of sediments and the bar clearance (from 0.18 to 0.83). Castillo *et al.* [11, 12] carried out numerical simulations with the computational fluid dynamics (CFD) methodology. They analyzed the increment in the wetted rack length due to the sediment transport. The authors considered different sediment concentrations (from 1.0 to 5.0% in volume), void ratios from 0.16 to 0.60, flow rates and rack slopes. Castillo *et al.* [13] analyzed the influence of gravels whose d_{50} value was close to the spacing between bars. Different longitudinal rack slopes, water flows and solids concentrations were used. Tests showed a reduction of the collected flow due to the occlusion of the rack. The reduction seems to be related with the longitudinal rack slope. The maximum efficiency was obtained with a slope of 30%.

In this work, the effective void ratios and the rack length have been defined by experimental measurements taking into account the occlusion effect of an inlet flow with gravels.

In the analysis of clear water flows, some simplifications are often assumed: the flux over the rack is one-dimensional, the flow decreases progressively, the hydrostatic pressure distribution acts over the rack in the flow direction, the energy level or energy head is considered constant along the rack.

Several researchers analyzed these simplifications by means of laboratory hydraulic models. Noseda [8] studied the clear water flow through different racks. The author defined an expression to calculate the discharge coefficient, valid for horizontal rack case and subcritical approximation flow:

$$C_q = 0.66 m^{-0.16} \left(\frac{h}{l} \right)^{-0.13} \tag{1}$$

where l refers to the distance between the centerline of two consecutive bars, m the void ratio, and h the height of water measured in the vertical direction.

According to Brunella *et al.* [15], the differences between measured and calculated water depth profiles generally appear in two regions: at the beginning of the rack and at the end of the rack, when wall friction effects are neglected. Differences at the beginning of the rack are due to the consideration of hydrostatic pressure distribution.

Righetti and Lanzoni [16] calculated the flow collected by the rack with the following differential equation:

$$dq(x) = C_q m \sqrt{2g(H_0 + \Delta z)} dx \qquad (2)$$

where m is the void ratio, dx the differential rack length in the flow direction, H_0 the total energy at the beginning of the rack, Δz the vertical distance between the edge of the rack and the analyzed section, and C_q the discharge coefficient. The same authors considered that $Cq \approx \sin \alpha$, with α being the angle between the velocity vector of water collected by the rack and the plane of the rack.

Several researchers proposed expressions to calculate the wetted rack length L required to collect a determined flow (Table 1).

Table 1: Formulations for flow profiles and wetted rack lengths (Castillo and Lima [17]).

Author	Formulation	Parameters
Bouvard [18], Bouvard and Kuntzmann [19]	$L = \left\{ \dfrac{1}{2.m''}\left[\left(j + \dfrac{1}{2.j^2}\right).\arcsin\sqrt{\dfrac{j}{j+(1/2.j^2)}} + 3\sqrt{\dfrac{1}{2.j}}\right] + \left(\dfrac{0.303}{m''^2} + \dfrac{2j^3 - 3.j^2 + 1}{4.j^2}\right)tg\varphi \right\}.h_1.\cos\varphi$ $j = \dfrac{h_1}{h_c}; \quad m'' = m.C_q$	h_1 = depth at the beginning of the rack; h_c = critical depth; m'' = product of the void ratio and the discharge coefficient
Noseda [8]	$L = \dfrac{E_0}{C_q.m}[\Phi(y_2) - \Phi(y_1)]; \quad \Phi = f(y); \quad y = \dfrac{h}{E}$ $L = 1.1848\,\dfrac{E_0}{C_q.m}$ $\Phi = \dfrac{1}{2}\arccos\sqrt{y} - \dfrac{3}{2}\sqrt{y(1-y)}$	E_0 = specific energy at the beginning of the rack
Frank [20]	$L = 2.561\dfrac{q_1}{\lambda\sqrt{h_1}}$ $\lambda = mC_{q0}.\sqrt{2.g.\cos\varphi}$ $C_{q0} = 1.22 C_{q_{x=x_0}}$	h_1 = depth at the beginning of the rack; q_1 = incoming specific flow; φ = angle of the rack with the horizontal plane
Krochin [14]	$L = \left[\dfrac{0.313 q_1}{(C_q k)^{3/2}}\right]^{2/3}; \quad k = (1-f)m; \quad f = 0.15 - 0.30$ $C_q = C_0 - 0.325 tg\alpha$ $C_0 = 0.6$ if m $\geq$ 4 $C_0 = 0.5$ if m $<$ 4	q_1 = incoming specific flow; f = obstruction coefficient

2   Materials and methods

2.1 Physical device

An intake system has been built at the Hydraulic Laboratory of the Universidad Politécnica de Cartagena. It consists of a 5.00 m long and 0.50 m wide approximation channel, a rack with different slopes (from horizontal to 33%), a discharge channel, and the channel to collect derived water. Figure 1 shows the water through the rack when gravels are tested.
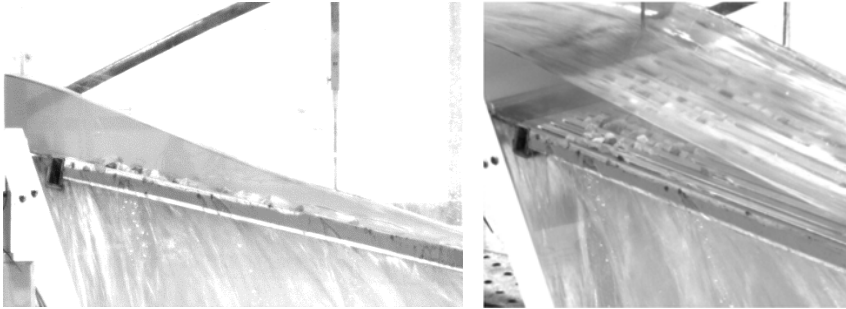

Figure 1:   Gravel test at the laboratory device of the Hydraulic Laboratory of Universidad Politécnica de Cartagena.

Tests with clear water have been done using three different racks with 0.9 m lengths. All of them are made of aluminum bars with T profiles (T 30/25/2 mm). The bars are disposed longitudinally to the inlet flow. The difference between the racks is the spacing between bars, so different void ratios are available. Table 2 summarizes the geometric characteristics of each rack.

Table 2:   Geometric characteristic of the tested racks.

	A	B	C
Spacing between bars (mm)	5.70	8.50	11.70
Void ratio $m = \dfrac{b_1}{b_1 + 30}$	0.16	0.22	0.28

Different specific flows (53.8, 77.0, 114.6, 138.88, and 155.4 l/s/m), and rack slopes (0%, 10%, 20%, 30%, 33%) have been considered. The inlet flow, q_1, is measured in an electromagnetic flowmeter at the beginning of the channel. The rejected flow, q_2, is measured by using a V-notch weir located in the channel that collects the rejected flow. The flow derived by the rack, q_d, is calculated as a difference between q_1 and q_2. In each test, the flow depth along the rack and the wetted rack length were measured.

To test the hydraulic behaviour of the intake system, the laboratory measurements were used to model and calibrate computational fluid dynamics (CFD) simulations. CFD codes solve the differential Reynolds-Averaged Navier–Stokes (RANS) equations of the phenomenon in the fluid domain, retaining the reference quantity in the three directions for each control volume identified. The equations for conservation of mass and momentum may be written as:

$$\frac{\partial \rho}{\partial t} + \frac{\partial}{\partial x_j}\left(\rho U_j\right) = 0 \qquad (3)$$

$$\frac{\partial \rho U_i}{\partial t} + \frac{\partial}{\partial x_j}\left(\rho U_i U_j\right) = -\frac{\partial p}{\partial x_i} + \frac{\partial}{\partial x_j}\left(2\mu S_{ij} - \rho \overline{u_i' u_j'}\right) \qquad (4)$$

where i and j are indices, x_i represents the coordinate directions ($i = 1$ to 3 for x, y, z directions, respectively), ρ the flow density, t the time, U the velocity vector, p the pressure, u_i' presents the turbulent velocity in each direction ($i = 1$ to 3 for x, y, z directions, respectively), μ is the molecular viscosity, S_{ij} the mean strain-rate tensor, and $-\rho \overline{u_i' u_j'}$ the Reynolds stress.

Eddy-viscosity turbulence models consider that such turbulence consists of small eddies which are continuously forming and dissipating, and in which the Reynolds stresses are assumed to be proportional to mean velocity gradients. The Reynolds stresses may be related to the mean velocity gradients and eddy viscosity by the gradient diffusion hypothesis:

$$-\rho \overline{u_i' u_j'} = \mu_t \left(\frac{\partial U_i}{\partial x_j} + \frac{\partial U_j}{\partial x_i}\right) - \frac{2}{3}\delta_{ij}\left(\rho k + \mu_t \frac{\partial U_k}{\partial x_k}\right) \qquad (5)$$

with μ_t being the eddy viscosity or turbulent viscosity, $k = 1/2\overline{u_i' u_i'}$ the turbulent kinetic energy and δ the Kronecker delta function.

The CFD volume finite scheme program ANSYS CFX (version 14.0) [21] has been used. The k-ω based Shear-Stress-Transport (SST) turbulence model was selected to complement the numerical solution of the Reynolds-averaged Navier–Stokes equations (RANS). To solve the two-phase air-water, the homogeneous model was used. The fluid domain is divided into control volumes, which must satisfy the balance of the governing equations. The total number of elements used in the simulations was around 350,000 elements, with 0.004 m length scale near the rack. For simplicity, it has been considered that all the longitudinal bars work in the same mode in the intake system. For this reason, the domain fluid considers three bars and two spacings between bars. Symmetry conditions were used in the central plane of the extreme bars.

The model boundary conditions correspond to the flow at the inlet condition (located 0.50 m upstream of the rack), the upstream and downstream water levels and their hydrostatic pressures distributions. In the bottom of the water collected channel, opening boundary conditions were used. It has been assumed that the free surface is on the 0.5 air volume fraction.

3 Results and discussion

3.1 Clear water experimental tests

We have compared the angle of the velocity vector of the water collected by the rack, with the horizontal plane. Righetti *et al.* [22] obtained in their lab studies that the range of this angle is between 25 and 35 degrees, reducing as the water depth decreases. The sinus of this angle may be used to estimate the discharge coefficient of the water collected through the rack.

Figure 2 shows the results obtained with numerical simulations using CFD simulations when rack C ($m = 0.28$) is tested. The inlet specific flow $q_1 = 155.4$ l/s/m and different slopes are analyzed. The angle tends to increase with the slope of the rack. Although the racks and flows are not the same as those used by Righetti *et al.* [22], the values obtained are in the same range as those observed in the lab, reducing the angle with the decreasing of the water depth over the rack.
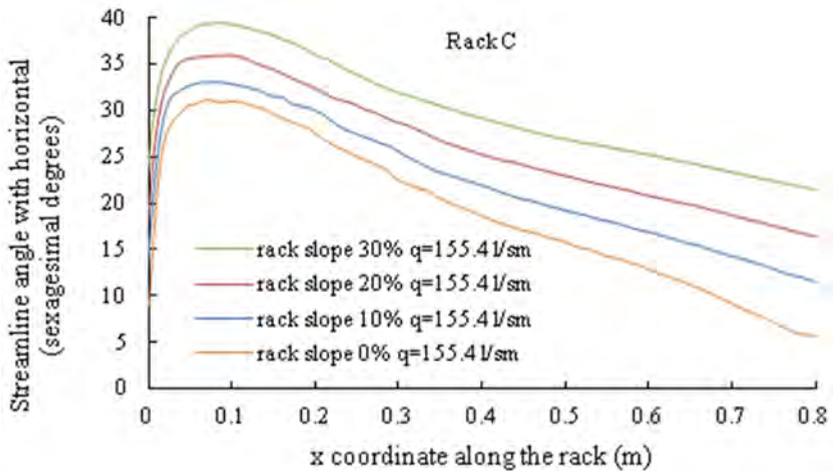

Figure 2:   Angle of velocity vector of water collected with the horizontal plane.

3.2 Sediment experimental tests

In order to evaluate the effect of the sediment transport over the rack, two gravel-size materials have been analyzed. The sieve curves are almost uniform. The average grain size is $d_{50} = 8.3$ mm for gravel 1 and $d_{50} = 14.8$ mm for gravel 2. Previous studies (Castillo *et al.* [13]) focused on the comparison of the results obtained in clear water and in water with gravel transport.

Racks B ($m = 0.22$) and C ($m = 0.28$) have been used to test the gravels transport. In rack B, tests were carried out using gravel 1, with three specific flows ($q_1 = 77.0$, 114.6 and 155.4 l/s/m), and five slopes ($i = 0$, 10, 20, 30 and 33%). In rack C, gravel 2, three specific flows ($q_1 = 114.6$, 138.88 and 155.4 l/s/m), and the same five slopes were studied.

Sediments were uniformly added at the beginning of the inlet channel. The inlet point of the sediments is located five meters upstream of the rack. The solid flow at the beginning of the channel was $q_s = 0.33$ kg/s. Hence, solid concentrations in volume at the inlet of the channel were between 0.16 and 0.34%, depending on the water flow tested.

Each condition was repeated twice. Tests were continued until all the solids reached the downstream side of the rack. The duration of the test was between 700 and 1620 seconds.

In the tests, the flows derived by the occluded racks have been measured. To define the effective void ratio in the occluded racks, m', a differential equation of constant energy head is numerically solved using the fourth-order Runge–Kutta algorithm. The system of equations is equivalent to the solution of two ordinary differential equations for $h(x)$ and $q(x)$. At the inlet section, two boundary conditions are considered: the inlet specific flow q_1 and the initial energy E_0 (estimated as the critical energy head). The discharge coefficient value is obtained with the eqn (1). The numerical computation interval for x is 0.05 m. The numerical results for $h(x)$ are successfully compared with clear water test data. The energy equation to obtain m' is

$$\frac{dh}{dx} = \frac{m'0.66m'^{-0.16}\left(\frac{h}{l}\right)^{-0.13} 2\sqrt{h\cos\alpha(E_0 - h\cos\alpha)}}{3h\cos\alpha - 2(E_0)} \tag{6}$$

$$\frac{dq}{dx} = -C_q m\sqrt{2gh\cos\alpha} \tag{7}$$

where α is the angle of longitudinal rack with horizontal.

Due to the gravel occlusion, wetted rack lengths calculated with effective void ratios have a bigger length than those obtained with clear water. This is more pronounced with the decrease of the rack slope. Other important variables are the inflow rate, q_1, and the gravel size.

From the inflow rate we can define the initial shear stress, τ_0, and Froude number, F_{r0}, values

$$\tau_0 = \gamma h_0 i; \quad F_{r0} = \frac{q_1}{g^{1/2} h_0^{3/2}} \tag{8}$$

where γ is the specific weight of water and h_0 the initial flow depth.

F_{r0} and τ_0 are calculated for each inflow condition, while q_1 and h_0 were measured at the beginning of the rack for each slope.

We can obtain some correlations: Figures 3 and 4 show the correlation between the effective void ratio, m', and the values of τ_0 and F_{r0}, when different rack slopes are considered. Figures 5 and 6 represent the ratio between the effective discharge coefficient, C_q', and the initials shear stress and Froude number.
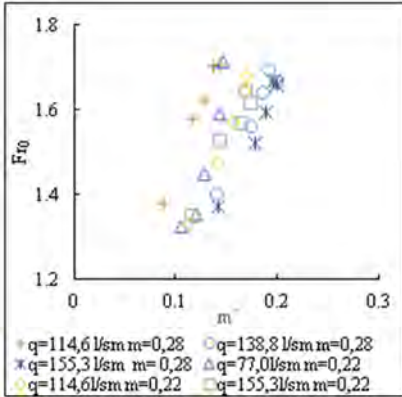
Figure 3: Correlation between the adjusted void ratio, m', and the initial Froude number, F_{r0}, for racks B and C, for different slopes and flow rates.
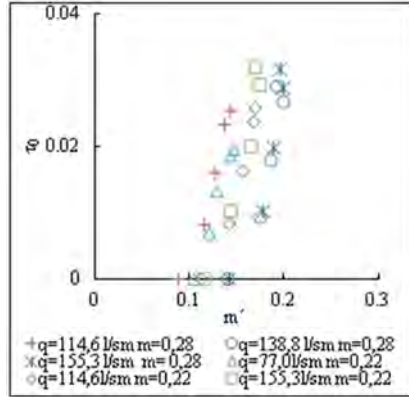

Figure 4: Correlation between the adjusted void ratio, m', and the initial shear stress, τ_0, for racks B and C, for different slopes and flow rates.
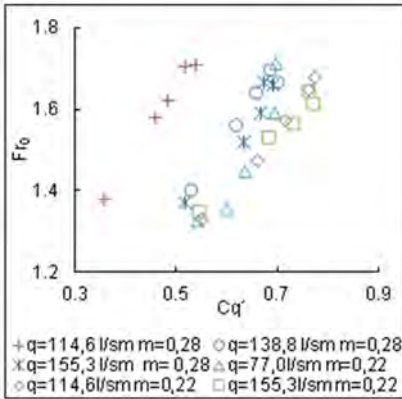

Figure 5: Correlation between the adjusted discharge coefficient, Cq', and the initial Froude number, F_{r0}, for racks B and C, for different slopes and flow rates.
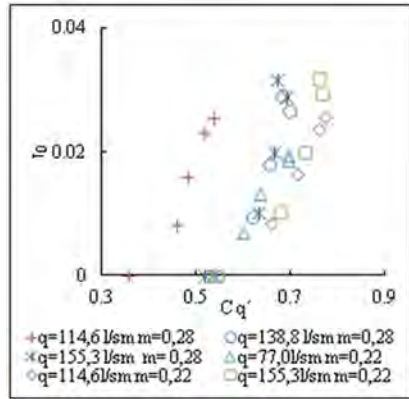

Figure 6: Correlation between the adjusted discharge coefficient, Cq', and the initial shear stress, τ_0, for racks B and C, for different slopes and flow rates.

An adjustment of the initial shear stress with the void adjusted by the occlusion effect may be proposed (Figure 7). The potential adjustment obtained with $R^2 = 0.994$ is

$$\tau_0 = 2.5496 \left[m'i^{0.46} + \left(0.004 F_{r0}\right)^{2.1} \right]^{1.9477} \tag{9}$$
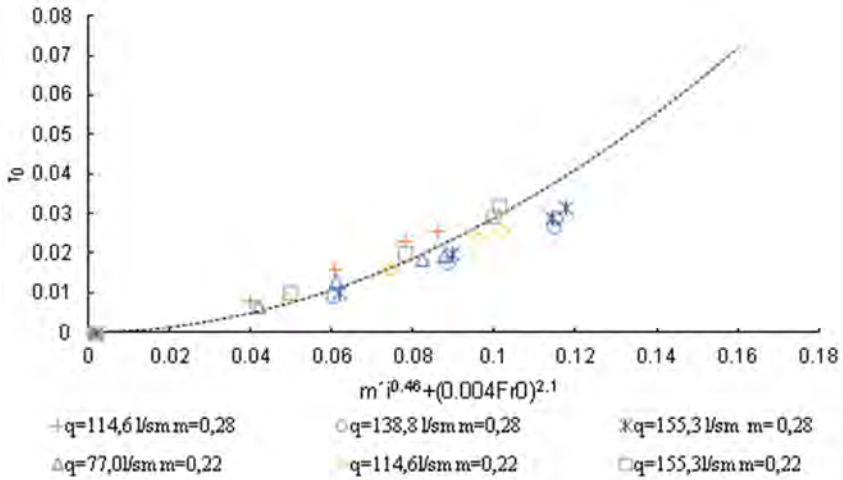
Figure 7:   Adjustment of void ratio to initial shear stress for racks B and C and different flow rates and slopes.

Figure 8 shows a comparison between the computed void ratio m' using eqn (9) with the experimental measurements. The computed void ratio is within $\pm25\%$ of the observed ones.
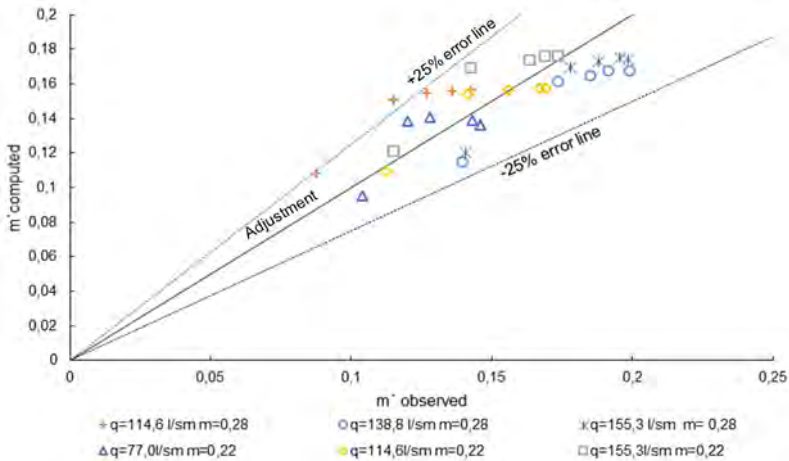

Figure 8:   Comparison of observed void ratio with computed.

To use eqn (9), the initial flow depth, h_0, and the inflow rate, q_1, should be known. Frank [7] proposed the initial flow depth, h_0, as a function of the longitudinal rack slope for different inflow rates. In Figure 9, eqn (9) has been used to compute the effective void ratio. Then, the wetted rack lengths have been obtained taking into account the occlusion due to gravels.
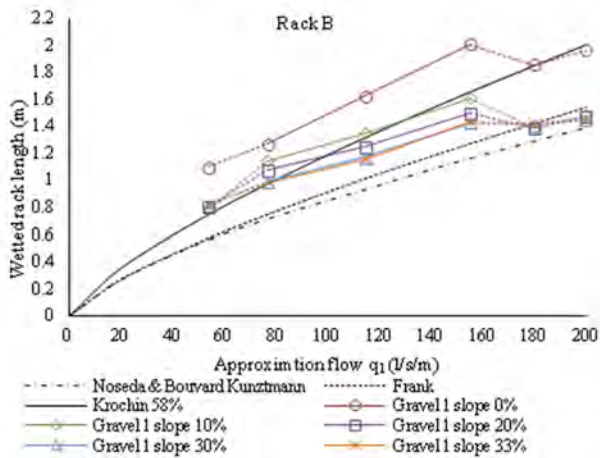

Figure 9:   Wetted rack lengths for rack B defined with experimental test and adjusted (dashed line) with eqn (9).

In clear water, the decrease in the approximation flow rate, q_1, results in a reduction of the wetted rack length. In tests with gravels, designers also need to consider the decrease in the effective void ratio, which tends to increase the wetted rack length. The prevalence of one of these opposite effects justifies the observed peaks in Figure 9.

4   Conclusions

In this work, bottom water intake systems are analyzed in order to utilize them in dry riverbeds. Since rain episodes are torrential in semiarid regions, the objective is to derivate the maximum amount of water with the minimum amount of sediment.

The shape and spacing between bars are parameters that need to be considered as a function of the materials existent in the river bed.

Clear water simulations solved with CFD code obtained a good agreement with experimental data, when several flows and rack slopes were considered.

The effective void ratio, and rack length are defined by experimental measurements of flows with gravel size sediment through bottom racks in which the occlusion effect appears. Preferential deposition zones along the rack are observed in laboratory.

A potential equation relating the shear stress at the beginning of the rack with effective void ratio is proposed. This allows researchers to calculate the increment of wetted rack length in case of gravels with a d_{50} value around or superior to the spacing between the bars.

Additional experimental tests should be carried out modifying the sieve curves, and using diverse rack conditions such as void ratios, slopes, and type of bars. In general, wetted rack lengths considering occlusion are in agreement with an obstruction coefficient of 58% in the Krochin [14] formulae.

Traditional design criteria of bottom rack systems in mountain rivers usually consider a bar clearance higher than d_{90}. This study enables to know the behaviour of bottom systems with a reduced bar clearance from the point of view of the occlusion.

References

[1]   Bouvard, M., Mobile Barrages & Intakes on Sediment Transporting Rivers. IAHR Monograph, Balkema, Rotterdam, 1992.
[2]   Ract-Madoux, M., Bouvard, M., Molbert, J., & Zumstein, J., Quelques réalisations récentes de prises en-dessous à haute altitude en Savoie. La Houille Blanche, 6, pp. 852-878, 1955.
[3]   Simmler, H., Konstruktiver Wasserbau, Technische Universität Graz. Institut für Wasserwirtschaft und konstruktiven Wasserbau, 1978.
[4]   Drobir, H., Entwurf von Wasserfassungen im Hochgebirge. Österreichische Wasserwirtschaft, 11(12): pp. 243-253, 1981.
[5]   Raudkivi, A.J., Hydraulic Structures Design Manual. IAHR, pp. 92-105, 1993.
[6]   Orth, J., Chardonnet, E. & Meynardi, G., Étude de grilles pour prises d'eau du type. La Houille Blanche, 9(6), pp. 343-351, 1954.
[7]   Frank, J., Hydraulische Untersuchungen für das Tiroler Wehr. Der Bauingenieur, 31(3): pp. 96-101, 1956.
[8]   Noseda, G., Correnti permanenti con portata progressivamente decrescente, defluenti su griglie di fondo. L'Energia Elettrica, pp. 565-581, 1956.
[9]   Drobir, H., Kienberger, V. & Krouzecky, N., The wetted rack length of the Tyrolean weir. Proc. of the 28th IAHR Congress, Graz, pp. 22-27, 1999.
[10]   Ahmad, Z. & Kumar S., Estimation of trapped sediment load into a trench weir, Proc. of the 11th International Symposium on River Sedimentation (ISRS), University of Stellenbosch, South Africa, pp. 1-9, 2010.
[11]   Castillo, L.G., Carrillo, J.M., & García, J.T., Comparison of clear water flow and sediment flow through bottom racks using some lab measurements and CFD methodology. Proc. of the Seven River Basin Management, Wessex Institute of Technology, 2013.
[12]   Castillo, L.G., Carrillo, J.M., & García, J.T., Flow and sediment transport through bottom racks. CFD application and verification with experimental measurements. Proc. of the 35th IAHR Congress, Chengdu, 2013.

[13]   Castillo, L.G., García, J.T., & Carrillo, J.M., Experimental measurements of flow and sediment transport through bottom racks. Influence of graves sizes on the rack. Proc. of the 7th Int. Conf. River Flow, Lausanne, 2014.

[14]   Krochin, S., Diseño Hidráulico. Segunda Edición. Colección Escuela Politécnica Nacional. Quito. Ecuador, 1978.

[15]   Brunella, S., Hager, W. & Minor, H., Hydraulics of Bottom Rack Intake. Journal of Hydraulic Engineering, 129(1), pp. 4-9, 2003.

[16]   Righetti, M. & Lanzoni, S., Experimental Study of the Flow Field over Bottom Intake Racks. Journal of Hydraulic Engineering, 134(1), pp. 15-22, 2008.

[17]   Castillo, L.G., & Lima, P., Análisis del dimensionamiento de la longitud de reja en una captación de fondo. Proc. of the XXIV Congreso Latinoamericano de Hidráulica, Punta del Este, 2010.

[18]   Bouvard, M., Debit d'une grille par en dessous. La Houille Blanche, 2: pp. 290-291, 1953.

[19]   Bouvard, M., & Kuntzmann, J., Étude théorique des grilles de prises d'eau du type "En dessous". La Houille Blanche, 5, pp. 569-574, 1954.

[20]   Frank, J., Fortschritte in der hydraulic des Sohlenrechens. Der Bauingenieur, 34, pp. 12-18, 1959.

[21]   ANSYS, Inc., ANSYS CFX-Solver Theory Guide. Release 14.0, 2011.

[22]   Righetti, M., Rigon, R., & Lanzoni, S., Indagine sperimentale del deflusso attraverso una griglia di fondo a barre longitudinali. Proc. of the XXVII Convegno di Idraulica e Costruzioni Idrauliche, Genova, pp. 112-119, 2000.